ADVANCED FUNCTIONAL MATERIALS

FULL PAPER

DOI: 10.1002/adfm.200500415

Nanoscale Effects on the Ionic Conductivity of Highly Doped Bulk Nanometric Cerium Oxide**

By *Umberto Anselmi-Tamburini*, *Filippo Maglia*, *Gaetano Chiodelli*, *Alessandra Tacca*, *Giorgio Spinolo*, *Pietro Riello*, *Stefania Bucella*, and *Zuhair A. Munir**

Nanometric ceria powders doped with 30 mol % samaria are consolidated by a high-pressure spark plasma sintering (HP-SPS) method to form > 99 % dense samples with a crystallite size as small as 16.5 nm. A conductivity dependence on grain size was noted: when the grain size was less than 20 nm, only one semicircle in the AC impedance spectra was observed and was attributed to bulk conductivity. In contrast to previous observations on pure ceria, the disappearance of the grain-boundary blocking effect is not associated with mixed conductivity. With annealing and concomitant grain growth, the samples show the presence of a grain-boundary effect.

1. Introduction

Modification of the electrical properties of oxides with grain size in the nanometric range has been the objective of many investigations in the past few years.[1–7] Most of these studies have focused on loose powders and thin films, with much less attention being given to bulk materials. This is due to the difficulties encountered in the production of fully dense bulk ceramic materials with a grain size in the nanometer range, particularly below 30 nm. The high temperatures required to fully densify nanometric ceramic powders produce a significant grain growth that leads to the destruction of the nanostructure.[6]

This becomes a major concern in view of reports, based on thin film results, indicating that potentially significant modifications in the electrical properties of bulk ionic materials are to be expected for grain sizes approaching 10 nm or below, with the appearance of mesoscopic and confinement effects.[8,9] Although there are a few reported successes,[7,10–12] the synthesis of fully dense bulk ceramic materials with grain sizes below 30 nm is still considered problematic. However, we recently developed a non-conventional densification technique, based on a high-pressure modification of the spark plasma sintering (SPS) apparatus,[13] which made it possible to obtain full densification of ceramic nanometric powders in a few minutes with no or very limited grain growth. In this paper we report on the electrical properties of highly doped cerium oxide (30 mol % samaria) densified using the high-pressure modification of the SPS (HP-SPS) technique to produce samples with a grain size of 16.5 nm and relative densities above 99 %.

Cerium oxide has been largely investigated as an alternative material to zirconia for medium-temperature applications in solid-state electrochemical devices.[14–18] Pure ceria is a mixed conductor with very limited technological interest, but solid solutions containing up to 30 mol % of rare earth elements (usually Y, Gd, or Sm) have ionic conductivity significantly higher than that of zirconia, although their stability at high temperatures in a reducing environment is inferior. Ceria has also been recently investigated as a model system for the study of the mechanism responsible of the grain-boundary blocking effect in ionic oxygen conductors.[12,19–24] In this regard ceria has the advantage (relative to zirconia) of retaining the fluorite structure for all levels of doping. However, nanometric bulk materials have been investigated only for the case of pure ceria or ceria containing a very low dopant level (< 0.2 mol %). Most of these investigations have been conducted on samples with a grain size above 30 nm and a relative density slightly above 90 %, with the notable exception of the work of Chiang et al.[11]

2. Results

Table 1 shows the values of grain size and density for 30 mol % samaria-doped ceria samples sintered under different conditions. Fully dense samples were obtained at 1000 °C when a pressure of 146 MPa was applied. The crystallite size

[*] Prof. Z. A. Munir, Prof. U. Anselmi-Tamburini
Department of Chemical Engineering and Materials Science
University of California
Davis, CA 95616 (USA)
E-mail: zamunir@ucdavis.edu
Prof. F. Maglia, Dr. A. Tacca, Prof. G. Spinolo
Department of Physical Chemistry, University of Pavia
Vle Taramelli, 27100 Pavia (Italy)
Dr. G. Chiodelli
IENI-CNR, Sezione di Pavia
Vle Taramelli 16, 27100 Pavia (Italy)
Prof. P. Riello, Dr. S. Bucella
Departiment of Physical Chemistry, University of Venice
Dorsoduro 2137-30121, Venice (Italy)

[**] This work has been partially supported by a MIUR-PRIN grant. It was also part of a MIUR-FISR project of the Italian CNR and was partially supported by the National Science Foundation (USA).

Table 1. Density and crystallite size of samaria-doped ceria sintered at different temperatures and pressures.

Sample	Sintering temperature [°C]	Sintering pressure [MPa]	Crystallite size [nm]	Relative density [%]
SPS1	1000	146	35	> 99
SPS3	850	146	17.6	91
SPS4	820	530	16.5	> 99

was 35 nm. Decreasing the temperature with the same applied pressure resulted in a decrease in crystallite size, but also in a significant reduction in density. An example of these samples was included in the investigation so as to evaluate the effect of residual porosity on the electrical properties of these nanometric materials. However, when the pressure was increased to 530 MPa, full densification was obtained at 820 °C with a crystallite size of 16.5 nm. Crystallite-size values obtained by scanning electron microscopy (SEM) and X-ray diffraction (XRD) are in good agreement. SEM images of fracture surfaces of the fully dense samples obtained with pressures of 146 MPa (at 1000 °C) and 530 MPa (at 820 °C) are shown in Figure 1.

In the sample sintered at 1000 °C, a significant discoloration was observed, producing samples with a dark-gray color (the normal color is yellow). Discoloration had also been observed previously in yttria-stabilized zirconia samples (from white to brown and black) densified in the SPS apparatus.[25] In that case the discoloration was attributed to oxygen deficiency resulting from the exceedingly low oxygen partial pressure in the graphite die at high temperatures. A similar explanation probably holds for the present sample, which, when annealed in pure oxygen at 700 °C for 15 h, becomes yellow in color. No evidence of modification in the sample microstructure was found as a result of this annealing.

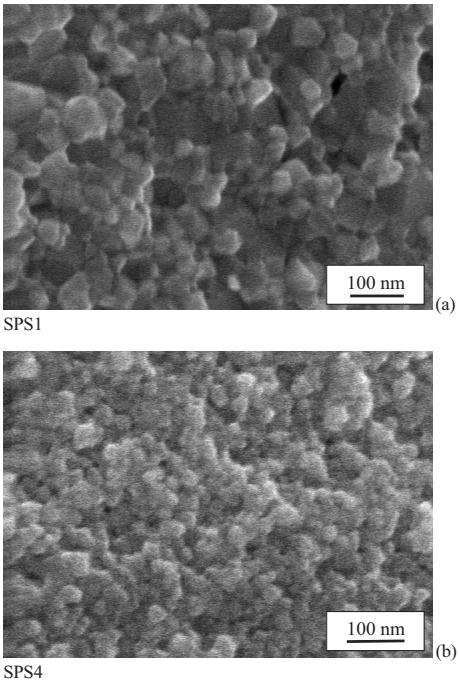

Figure 1. High-resolution SEM images of fracture surfaces of the samples SPS1 (a) and SPS4 (b).

Figure 2 shows the AC impedance spectra measured at 200 °C for the three samples reported in Table 1. For each sample, the spectra obtained before and after annealing at

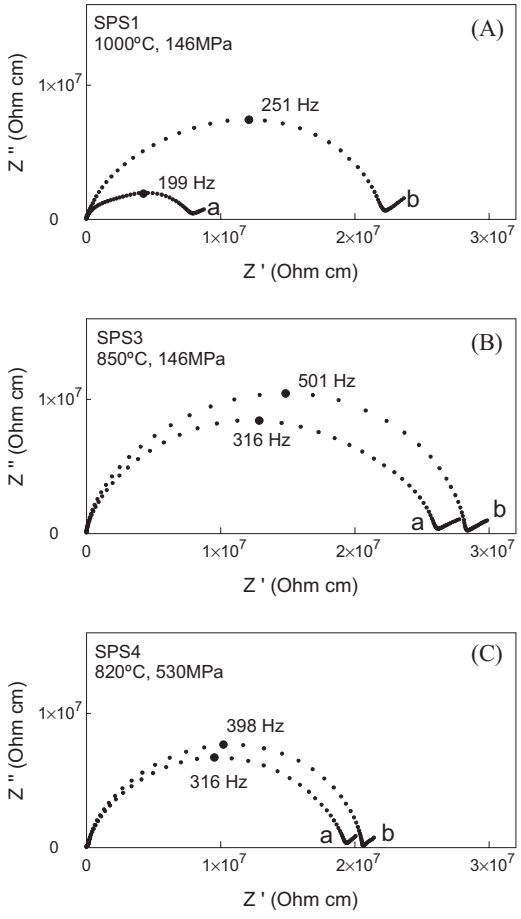

Figure 2. Impedance spectra for A) SPS1, B) SPS3, and C) SPS4. For all cases, the spectra labeled (a) and (b) are of the as-prepared sample and after annealing at 700 °C in pure oxygen for 10 h, respectively. All patterns were acquired at 200 °C.

700 °C in oxygen for 15 h are shown and labeled as "a" and "b", respectively. Only the sample densified at 1000 °C shows a significant variation in the spectrum as a result of the oxygen annealing. The other two samples show relatively minor changes. The most significant observation, however, is that all the patterns show only one, slightly deformed semicircle. Ceramic materials usually show two semicircles in their impedance spectrum: one at higher frequencies corresponding to transport phenomena in the bulk and one at lower frequencies related to transport phenomena at the grain boundary.[15–19] The low-frequency intercept on the real axis corresponds also to the total resistivity of the material.

Figure 3 shows an enlargement of the portion at low impedance (high frequency) of the data corresponding to the sample with the smaller grain size (SPS4), reported in Figure 2C. The

ADVANCED FUNCTIONAL MATERIALS

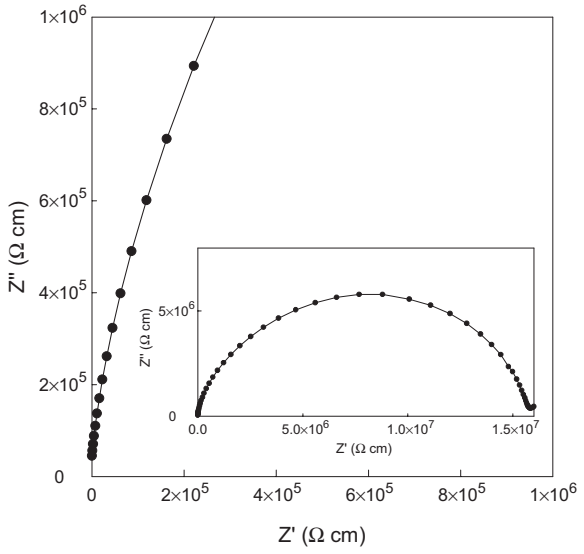

Figure 3. Enlarged portion of the high-frequency region of the AC impedance spectum for SPS4 reported in Figure 2C (curve b).

entire spectrum is reported in the inset. The figure shows clearly the absence of any other semicircle even at very high frequencies.

No significant change in the shape of the semicircle is observed in the sample sintered at 850 °C and 146 MPa (Fig. 2B), despite the presence of about 10 % of porosity. The absolute value of the total resistivity is increased, but the absence of a clear distinction between bulk and grain-boundary components in the AC impedance graphs does not allow for the evaluation of the contribution of porosity to the overall resistivity.

The dependence of the total resistivity measured under different oxygen partial pressures (at 700 °C) for the sample sintered at 820 °C and 530 MPa (SPS4, 16.5 nm) is shown in Figure 4. No variation in the resistivity was observed in the range $1 > p_{O_2} > 10^{-8}$ atm (1 atm = 101 325 Pa) at 700 °C. This result confirms that the material remains a fully ionic conductor even at fairly low oxygen partial pressures.

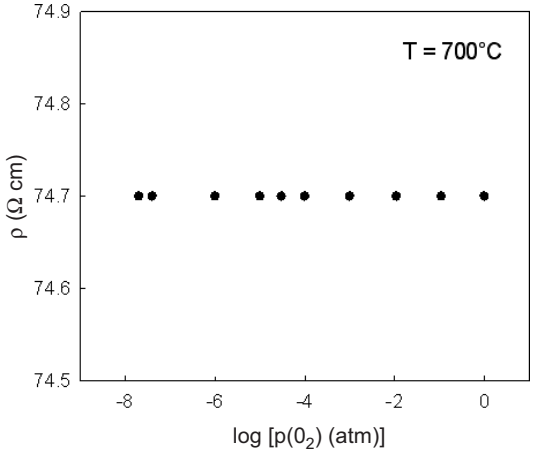

Figure 4. Total resistivity at 700 °C of SPS1 as a function of the oxygen partial pressure.

Figure 5 shows the dependence of the total conductivity on temperature for the two fully dense samples reported in Table 1. For reference, two other sets of data are also shown in Figure 5. One is for the microcrystalline sample obtained with the traditional ceramic method, as described in the Experimental Section, the second set is taken from the work of Jung et al.[16] for a sample with 30 mol % samaria. The values for the activation energy, E_a, and pre-exponential factor, A, for these samples are reported in Table 2. The activation energies are very similar for all samples with magnitudes close to 1 eV, a value often reported in the literature for highly doped ceria.[16] It is important to note that the conductivities reported in Figure 5 for the reference samples are only for the bulk component (i.e., excluding the grain-boundary contribution) while those from our nanometric samples are the total conductivities. In other words, the total conductivity of our samples is very similar to, or even higher than, the bulk conductivities in microcrystalline samples. Table 2 also shows values of the relative dielectric constants, ε_r. The reported values appear to be compatible with a bulk ceramic material like ceria.[24,26]

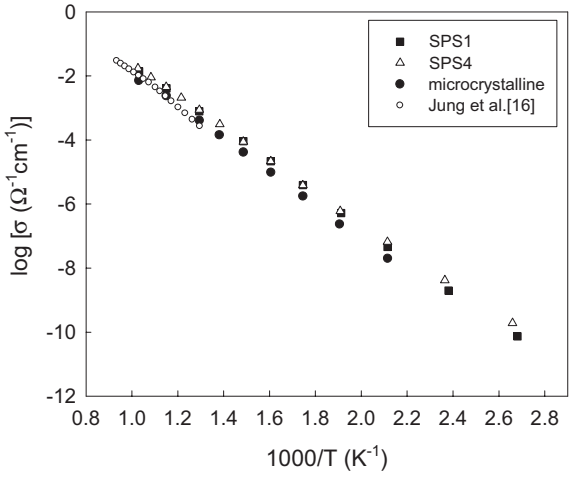

Figure 5. Arrhenius plot for the total electrical conductivity of samples SPS1 and SPS4. The conductivity of a microcrystalline reference sample and the results from Jung et al. [16] for the same composition are also shown. In these last two cases the reported values refer only to the bulk conductivity.

Table 2. Activation energies for conductivity of samaria-doped ceria

Sample	Densification temperature [°C]	E_a [eV]	A [ohm^{-1} cm^{-1}]	α
SPS1	1000	0.98	1.2×10^{-3}	58.8
SPS3	850	1.00	2.8×10^{-3}	51.0
SPS4	820	0.99	2.2×10^{-3}	60.0
Microcrystalline	1300	1.053	4.6×10^{-3}	25.0

The sample sintered at 1000 °C (SPS1) was annealed in air at 1200 and 1300 °C for 24 h. Upon annealing, the grain size of the sample increased from 35 to 400 nm. The relative evolution in the impedance spectrum measured at 200 °C is shown in Figure 6b–d. The impedance pattern of the sample sintered at 820 °C and 530 MPa (SPS4, 16.5 nm) is shown in Figure 6a. As a result, the figure reports patterns for samples with crystallite size ranging from 16.5 to 400 nm. As the crystallite sizes increases a second semicircle at lower frequencies appears. After annealing at 1300 °C for 24 h, the spectrum resembles the impedance pattern of a typical ceramic material with two well-resolved semicircles to be attributed to the bulk and to the grain boundary.

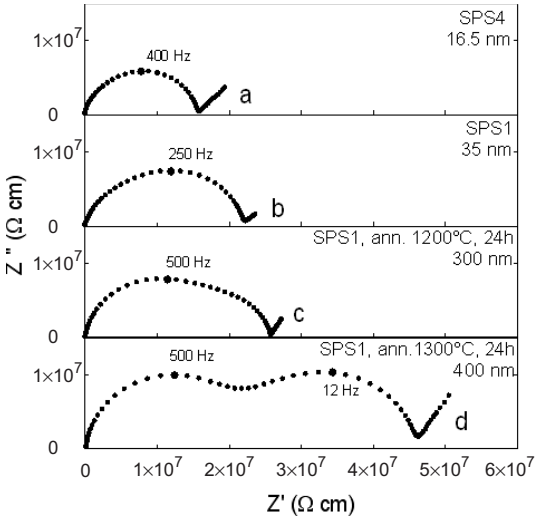

Figure 6. Impedance spectra of a) SPS4, b) SPS1 as-prepared, c) SPS1 annealed at 1200 °C for 24 h, and d) SPS1 annealed at 1300 °C for 24 h. All the patterns have been measured at 200 °C.

3. Discussion

The nature of the grain-boundary blocking effect in solid-state electrolytes has been the object of numerous investigations.[19–24,27–33] These studies have been motivated by the observation that grain boundaries contribute significantly to the overall resistance; in some cases this contribution is the main part of the total.

Three main mechanisms have been proposed to explain the grain-boundary blocking effect.[28,29] Two of these, impurity segregation and conduction restriction, involve the presence of a second phase (or porosity) at the grain boundary. But recent investigations have shown that even in very pure materials the specific grain-boundary resistivity can be several orders of magnitude higher than the bulk conductivity. To explain this behavior a third mechanism, based on the presence of a charge at the grain-boundary core and space-charge layers in the adjacent regions has been proposed. This space-charge model has been investigated experimentally and theoretically for the cases of zirconia and ceria.[8,12,19–24,33] However, none of these investigations has dealt with highly doped electrolytes with crystallite sizes in the low nanometer range.

The most striking result we observed in our samples is the presence of only one semicircle in the impedance spectroscopy data when the grain size is below 20 nm. As we have pointed out above, ceramic materials generally show the presence of two semicircles: one at high frequencies, usually associated with the transport in the bulk, and one at lower frequencies which is related to the grain boundary. The presence of only one semicircle does not necessarily indicate that only one of the two transport processes is present. Interpretation of impedance data requires careful consideration, particularly when materials with extreme mircostructure are considered. The two semicircles can be, at times, very different in size making one of the two difficult to detect, or they can overlap, as a result of the similar relaxation times for the two conduction processes. Our results, however, seem to exclude these possibilities and suggest that a single conduction mechanism, with characteristics very similar to the regular bulk conduction is active in the sample. Figure 3 shows the absence of any detectable second semicircle even in the extreme high-frequency region, where a second small semicircle can sometimes be observed when the grain-boundary resistivity is largely dominant. This suggests that the observed semicircle is associated with bulk and not to grain-boundary conduction. This conclusion is supported by the resistivity value, which is very similar to the value observed for bulk conduction in reference materials with the same composition[14–18] (see Fig. 5), and by the dielectric-constant value, which is in the range expected for bulk ceria, between 30 to 60 (see Table 2).[24]

The disappearance of the grain-boundary blocking effect has been reported before, but not in bulk materials with pure ionic conductivity. It has been observed in mixed conductors such as titanium oxide,[8] pure (undoped) cerium oxide,[11] and barium titanate,[34] and also in thin films.[35] The mechanism responsible for the disappearance of the grain-boundary blocking effect in these materials has been recently elucidated by Kim et al.[12,23,24] and Tschöpe et al.[20,21] on the basis of the space-charge model. In these materials the nanostructure produces a significant increase in the number of associated electrons. Due to the presence of a positive charge localized in the grain-boundary core, the electrons tend to be confined in the space-charge region. When the concentration of these electrons is sufficiently high the electronic conduction along the grain boundary can bypass the bulk ionic conduction. In this condition the blocking effect due to the grain boundaries disappears and a single semicircle is observed in the impedance spectrum. This mechanism, however, cannot be invoked in the case of pure ionic conductors like highly doped ceria. Our results show that such ionic behavior is not modified by the nanostructure in our sample. No dependence of the electrical conductivity on oxygen partial pressure is observed (Fig. 4). Furthermore, the temperature dependence of the conductivity (Fig. 5) is very similar to the one observed for the bulk ionic conductivity in micrometric sintered materials with activation energy values corresponding to values reported in the literature (around 1 eV).

In many aspects the electrical properties of the bulk nanometric material we produced are very similar to the ones ob-

ADVANCED FUNCTIONAL MATERIALS

served in a single crystals despite the fact that the grain size is close to 10 nm and a considerable fraction of the atoms are located in or in the vicinity of the grain boundary. The total conductivity of our nanometric material is even slightly higher that the bulk conductivity of a regular microcrystalline material, particularly at lower temperatures (Fig. 5).

As was shown above, when the nanometric samples are annealed at high temperature a second semicircle at lower frequencies appears. This new semicircle has all the characteristics of a regular grain-boundary contribution as its activation energy is just slightly higher that the one for the bulk (for the sample SPS1 annealed at 1300 °C for 24 h, $E_b = 1.096$, $E_{gb} = 1.104$), a behavior very similar to the one reported for grain-boundary contribution in regular micrometric material with high levels of doping. The small difference observed between the two activation energies rules out the possibility that the appearance of a grain-boundary contribution be related to a segregation of a second phase at the grain boundary. For that, a bigger difference in the activation energy would be expected. The presence of a current constriction effect produced by a second phase can also be excluded due to the high purity of the material and the extremely small grain size. A very large amount of a second phase would be necessary in order to produce a similar effect.

At this stage, only tentative explanations for the behavior of our nanometric materials can be proposed. Quite likely an interpretation must be found in the framework of the space-charge model. In the classical formulation of this model,[30] the source of the grain-boundary blocking effect in purely ionic conductors is the depletion of oxygen vacancies in the proximity of the grain-boundary core. This depletion is the result of a positive charge located at the grain-boundary core itself that repels the positively charged oxygen vacancies ($V_O^{\bullet\bullet}$). At the low sintering temperatures we used for our samples (< 1000 °C) the mobility of the substitutional atoms (Sm_{Ce}') is extremely small. As a result, a uniform dopant distribution can be assumed across the grain boundary (Mott–Schottky approximation).[23,30] Using this approximation and assuming a dilute solution behavior, the ratio between the bulk conductivity (σ_{bulk}) and the grain-boundary conductivity (σ_{gb}) can be related to the grain-boundary core potential ($\Delta\varphi(0)$) through the relation:[23,30]

$$\frac{\sigma_{bulk}}{\sigma_{gb}} = \frac{\exp(2e\Delta\varphi(0)/kT)}{4e\Delta\varphi(0)/kT} \quad (1)$$

where e is the electronic charge, T is temperature, and k is the Boltzmann constant. This relation shows that the ratio $\sigma_{bulk}/\sigma_{gb}$ decreases as $\Delta\varphi(0)$ decreases, and for very low potentials the ratio of the conductivities approaches unity and the grain-boundary blocking effect simply disappears. However, the source of $\Delta\varphi(0)$ is still unclear as it is dependence on the other parameters, such as dopant concentration and grains size. In the classical formulation of the space-charge model $\Delta\varphi(0)$ is an external parameter. Guo et al.[31] recently interpreted the drastic increase in the specific grain-boundary conductivity observed in microcrystalline yttria-doped ceria with an actual decrease in $\Delta\varphi(0)$. On the other side, Guo and Zhang,[32]Anselmi-Tamburini et al.,[25] and Aoki et al.[36] have observed a significant increase in the specific grain-boundary conductivity in yttria-doped zirconia, when the grain size decreases in the nanometer range. On the basis of these observations, we can argue that when a high level of doping and very small grain size are achieved, a substantial decrease in the value of $\Delta\varphi(0)$ is obtained, with a consequent disappearance of the grain-boundary blocking effect. Whether this is related to the very small grain size or to a non-equilibrium defect distribution promoted by the very low sintering temperature we used is unclear and cannot be clarified by annealing experiments (Fig. 6), as in these experiments both grains-size growth and defect annealing occur.

4. Conclusions

Nanometric powders (with a grain size of 10.8 nm) of cerium oxide doped with 30 mol % samaria, synthesized by a wet-chemistry method, were consolidated by a modified SPS method. The method uses a combination of a high-density pulsed DC current and a uniaxial pressure to sinter materials. The modification of the SPS allowed us to achieve pressures as high as 1 GPa. The density of the samaria-doped ceria samples depended on pressure, but more importantly, the pressure had a strong effect on grain size. When a pressure of 530 MPa was used, full densification (>99 % relative density) was obtained at 820 °C. The crystallite size was 16.5 nm. The samples were characterized using AC impedance measurements and the results showed a dependence on grain size. When the grain size was less than 20 nm, only one semicircle in the impedance spectroscopy was observed and was attributed to bulk conductivity. This conclusion was supported by resistivity and dielectric constant values, which were consistent with bulk conduction for this material. Thus, the results show the absence of the grain-boundary blocking effect, the disappearance of which has been reported before but not in bulk materials with pure ionic conductivity, which is the case in this study. A tentative explanation for the observed behavior of this material is proposed and is based on the space-charge model. It is proposed that with a high doping level in a material with very small grain size, the potential at the core of the grain boundary decreases significantly. The concomitant decrease in oxygen vacancies in the space-charge region associated with this leads to the disappearance of the grain-boundary blocking effect, as has been proposed for purely ionic conductors.

5. Experimental

Samaria-doped ceria powders were synthesized using a wet-chemistry method. Cerium nitrate hexahydrate (99.99 %, Aldrich), samarium nitrate hexahydrate (99.9 %, Aldrich), and ammonia solution 30 % (RPE, Carlo Erba) were used for the synthesis. Ammonia was slowly added to the Ce/Sm water solution (final concentration 0.1 M) while keeping the pH at a constant value of nine during the precipitation. After aging at room temperature for 1 h, the precipitate was recovered by centrifuging and then washed with deionized water and dried at 110 °C. The powder was then annealed at 600 °C for 12 h. A heating rate of 20 °C min^{-1} and a cooling rate of 4 °C min^{-1} were used for this treatment. The phase composition and the grain size of the powder were determined using XRD. The powders were single-phase ceria

with lattice constants appropriate for their composition. The grain size was 10.8 nm. The powders were largely agglomerated with the size of agglomerates being several micrometers.

The densification of these powders was performed in a SPS apparatus (Sumitomo, model 1050). The SPS apparatus has some similarities with a conventional hot press. In the case of SPS, however, the heating is obtained through a passage of a pulsed high-current, low-voltage DC current directly through the graphite die that contains the sample [37,38]. The pulses are 3.3 ms in length, with a maximum voltage in the range 0–10 V and a peak current of several thousand amperes. The pulses are delivered in groups of up to 99 consecutive pulses, followed by 1–9 missing pulses. The whole sequence is commonly referred as a "pulse pattern" and is indicated by two numbers separated by a colon, with the first number indicating the number of pulses on, and the second the number of pulses off. In all our samples the pulse pattern used was 12:2. The densification was performed using two different approaches. A graphite die with an internal diameter of 19 mm, having a maximum operating pressure of 150 MPa, was used for the densification of the sample that resulted in a grain size of 35 nm. Smaller grain sizes were obtained using higher pressures (up to 530 MPa) and lower temperatures. A double acting die with high-pressure components made with SiC and tungsten carbide was used in this case, as described elsewhere [13]. The samples had a diameter of 5 mm and a thickness of 1.5 mm. For all samples a heating rate of 200 °C min^{-1} and a hold time at the defined sintering temperature of 5 min were used. A vacuum of 0.1 Torr (1 Torr = 133.322 Pa) was maintained in the apparatus during all the experiments. The temperatures were measured using a shielded K-type thermocouple inserted in the lateral wall of the die. The actual sample temperature was determined though a calibration curve obtained by placing a second thermocouple in the center of the sample.

A reference material with the same composition was prepared using traditional ceramic methods. CeO_2 and Sm_2O_3 (Alfa Aesar) were mixed and uniaxially pressed to form a pellet that was fired at 1200 °C for 20 h, ground, and fired again at 1200 °C for 20 h. After final grinding the powder was isostatically pressed at 300 MPa and sintered at 1400 °C for 15 h.

Densities of the samples were determined using either the Archimedes method or by means of geometric and gravimetric measurements. Microstructural characterization of the samples was made using a high-resolution SEM (Philips XL30s) equipped with a field-emission gun and operated at 5 kV and 200 nA. No conductive coating was applied on the fracture surface. The grain size was determined from SEM images of the fracture surfaces measuring 100 grains or more for each image. This procedure has been chosen as the more reliable after an accurate evaluation of all possible alternatives. The determination of grain size in ceramic materials below 20 nm is particularly challenging and no generally accepted procedure is available [13]. Most of the traditional and well-established ceramographic techniques cannot be used in materials in this range of grain size. Thermal etching of polished surfaces cannot be performed because the high temperatures required by this process can produce significant grain growth (see the literature for example [39]). The procedure we used, however, produced very consistent results, generally in very good agreement with results obtained using X-ray diffraction.

Powder X-ray diffraction (XRD) analyses were performed using a Philips 1710 diffractometer equipped with a copper anode operated at 40 kV and 35 mA, graphite curved monochromator on the diffracted beam, and a proportional counter. The crystallite sizes were determined through analyses of XRD line broadening, using a published program [40,41] and sintered silicon as a standard. This procedure took into account the instrumental broadening and the presence of microstrain.

AC impedance characterization was performed using a Solartron 1260 frequency response analyzer in the frequency range between 10^{-3} Hz and 10 MHz. A voltage of 50–500 mV was used. In order to increase the sensitivity of the analyzer and reduce noise and capacitance effects of the cables and the cell a homemade high-impedance adaptor (10^{13} Ω, 3 pF) with an active guard was used [42]. The measuring apparatus was interfaced with a computer for data acquisition and manipulation. Platinum electrodes were deposited by sputtering on the flat surfaces of the pellets in order to ensure good electrical contact. The frequency dispersion measurements of the samples were obtained in controlled atmospheres, with an oxygen partial pressure ranging from 1 to 10^{-8} atm. The oxygen partial pressure was controlled using a system based on an electrochemical oxygen pump. The samples were kept at each partial pressure for a sufficiently long time to ensure that the resistance remained constant for at least 2 h. At the lowest oxygen partial pressures, an anneal time of at least 15 h was used.

Received: July 4, 2005
Revised: February 21, 2006
Published online: November 3, 2006

[1] P. Moriarty, *Rep. Prog. Phys.* **2001**, *64*, 297.
[2] H. Gleiter, *Acta Mater.* **2000**, *48*, 1.
[3] M. Cain, R. Morrell, *Appl. Organomet. Chem.* **2001**, *15*, 321.
[4] P. Knauth, *J. Solid State Electrochem.* **2002**, *6*, 165.
[5] J. Schoonman, *Solid State Ionics* **2000**, *135*, 5.
[6] C. P. Cameron, R. Raj, *J. Am. Ceram. Soc.* **1988**, *71*, 1031.
[7] H. L. Tuller, *Solid State Ionics* **2000**, *131*, 143.
[8] J. Maier, *Solid State Ionics* **2003**, *157*, 327.
[9] N. Sata, K. Eberman, J. Maier, *Nature* **2000**, *408*, 946.
[10] P. Knauth, H. L. Tuller, *J. Appl. Phys.* **1999**, *85*, 897.
[11] Y. M. Chiang, E. B. Lavik, I. Kosacki, H. L. Tuller, J. Y. Ying, *Appl. Phys. Lett.* **1996**, *69*, 185.
[12] S. Kim, J. Maier, *J. Eur. Ceram. Soc.* **2004**, *24*, 1919.
[13] U. Anselmi-Tamburini, J. E. Garay, Z. A. Munir, *Scr. Mater.* **2006**, *54*, 823.
[14] V. V. Kharton, F. M. B. Marques, A. Atkinson, *Solid State Ionics* **2004**, *174*, 135.
[15] K. Eguchi, T. Setoguchi, T. Inoue, H. Arai, *Solid State Ionics* **1992**, *52*, 165.
[16] G. B. Jung, T. J. Huang, C. L. Chang, *J. Solid State Electrochem.* **2002**, *6*, 225.
[17] S. Zha, C. Xia, G. Meng, *J. Power Sources* **2003**, *115*, 44.
[18] G. Chiodelli, G. Flor, M. Scagliotti, *Solid State Ionics* **1999**, *91*, 109.
[19] A. Tschöpe, S. Kilassonia, R. Birringer, *Solid State Ionics* **2004**, *173*, 57.
[20] A. Tschöpe, E. Sommer, R. Birringer, *Solid State Ionics* **2001**, *139*, 255.
[21] A. Tschöpe, *Solid State Ionics* **2001**, *139*, 267.
[22] A. Tschöpe, C. Bäuerle, R. Birringer, *J. Appl. Phys.* **2004**, *95*, 1203.
[23] S. Kim, J. Fleig, J. Maier, *Phys. Chem. Chem. Phys.* **2003**, *5*, 2268.
[24] S. Kim, J. Maier, *J. Electrochem. Soc.* **2002**, *149*, J73.
[25] U. Anselmi-Tamburini, J. E. Garay, Z. A. Munir, A. Tacca, F. Maglia, G. Chiodelli, G. Spinolo, *J. Mater. Res.* **2004**, *19*, 3263.
[26] J. H. Hwang, D. S. Mclachlan, T. O. Mason, *J. Electroceram.* **1999**, *3*, 7.
[27] D. Y. Wang, A. S. Nowick, *J. Solid State Chem.* **1980**, *35*, 325.
[28] K. El Adham, A. Hammou, *Solid State Ionics* **1983**, *9*, 905
[29] J. Jamnik, J. Maier, *Solid State Ionics* **1999**, *119*, 191.
[30] X. Guo, J. Majer, *J. Electrochem. Soc.* **2001**, *148*, E121.
[31] X. Guo, W. Sigle, J. Maier, *J. Am. Ceram. Soc.* **2003**, *86*, 77.
[32] X. Guo, Z. Zhang, *Acta Mater.* **2003**, *51*, 2539.
[33] X. Guo, R. Waser, *Prog. Mater. Sci.* **2006**, *51*, 151.
[34] X. Guo, C. Pithan, C. Ohly, C. L. Jia, J. Dornseiffer, F. H. Haegel, R. Waser, *Appl. Phys. Lett.* **2005**, *86*, 082 110.
[35] X. Guo, E. Vasco, S. Mi, K. Szot, E. Wachsman, R. Waser, *Acta Mater.* **2005**, *53*, 5161.
[36] M. Aoki, Y. M. Chiang, I. Kosacki, J. R. Lee, H. Tuller, Y. Liu, *J. Am. Ceram. Soc.* **1996**, *79*, 1169.
[37] W. Chen, U. Anselmi-Tamburini, J. E. Garay, J. R. Groza, Z. A. Munir, *Mater. Sci. Eng. A* **2005**, *394*, 132.
[38] U. Anselmi-Tamburini, S. Gennari, J. E. Garay, Z. A. Munir, *Mater. Sci. Eng. A* **2005**, *394*, 139.
[39] J. Kanters, U. Eisele, H. Böder, J. Rödel, *Adv. Eng. Mater.* **2001**, *3*, 158.
[40] S. Enzo, G. Fagherazzi, A. Benedetti, S. Polizzi, *J. Appl. Crystallogr.* **1988**, *21*, 536.
[41] A. Benedetti, G. Fagherazzi, S. Enzo, M. Battagliarin, *J. Appl. Crystallogr.* **1988**, *21*, 543.
[42] G. Chiodelli, P. Lupotto, *J. Electrochem. Soc.* **1991**, *138*, 2703.